J. Physiol. (1979), **295**, *pp.* 323–343
With 9 text-figures
Printed in Great Britain

A MATHEMATICAL MODEL FOR CONDUCTION OF ACTION POTENTIALS ALONG BIFURCATING AXONS

BY I. PARNAS AND I. SEGEV

From the Neurobiology Unit, the Hebrew University, Jerusalem, Israel

(*Received 4 August 1978*)

SUMMARY

1. A mathematical model based on the Hodgkin–Huxley equations is derived to describe quantitatively the propagation of action potentials in a branching axon.

2. The model treats the case of a bifurcating axon with branches of different diameters. The solution takes into account the changes in space constant in the different regions.

3. The model allows for investigating parameters leading to preferential conduction of action potentials in one daughter branch as seen experimentally.

4. Assuming that the only difference between the various daughter branches is in their diameters, conduction blocks should occur simultaneously rather than differentially into all daughter branches when the geometrical ratio is > 10.

5. In order to obtain differential conduction into the two branches changes in ionic concentrations due to the repetitive action potentials had to be introduced into the equations.

6. We find that conditions which allow differential buildup of K concentration around the two branches, produce differential conduction block. These conditions may be different periaxonal spaces around the branches or different time constant for recovery processes that eliminate K from the periaxonal space.

7. The effects of an inexcitable branch on conduction of action potentials in the second branch are described.

8. We find that the membrane current which is associated with the action potential is much more sensitive than the action potential itself and shows more distinct changes near regions of inhomogeneity such as a branch point, a step increase in diameter or an inexcitable branch.

INTRODUCTION

In the preceding papers (Grossman, Parnas & Spira, 1979*a*, *b*) we demonstrated that, contrary to the predictions of theoretical models (Goldstein & Rall, 1974), propagation of action potentials through a branch point that is geometrically equivalent to an unbranched axon of constant diameter fails at high frequencies. Furthermore, this failure does not occur at the same time for each branch; conduction into the larger branch is blocked sooner. The experimental results suggest that conduction failure and the differential channeling of impulses into the daughter axons may arise from changes in intracellular ion concentration (Na^+, Ca^{2+}) and extracellular accumulation of K (Grossman *et al.* 1979*b*; Spira, Yarom & Parnas, 1976; Parnas, 1979).

0022-3751/79/5130-0672 $01.50

In the present work, a mathematical model based on the Hodgkin & Huxley (1952) and Parnas, Hochstein & Parnas (1976) equations is derived to understand quantitatively some of the mechanisms which may allow differential propagation of action potentials along an axon with a geometrical inhomogeneity (branching, di:meter changes) and non-uniform membrane properties. The model allows us to investigate parameters leading to preferential conduction of action potentials in one of the daughter branches of a bifurcating axon, taking into account the effects of K accumulation in the periaxonal space and different rates of recovery mechanisms (Grossman *et al.* 1979*a*, *b*). We also examine the effect of an inexcitable branch on the propagation of action potentials at the segment of branching. A preliminary report on part of this work has been published (Segev & Parnas, 1977).

METHODS

List of symbols

a_j	Radius of segment j (cm)
a_j^S	(a_j^B) radius of branch S (B) at segment j (cm)
C	membrane specific capacitance (1 μF/cm^2)
C_j	capacitance of segment j (μF)
G_K	K conductance (mmho/cm^2)
G_L	leak conductance (mmho/cm^2)
G_{Na}	Na conductance (mmho/cm^2)
GR	the geometrical ratio of axon branches
h	Hodgkin & Huxley variable describing Na inactivation
I_C	density of capacitance current (μA/cm^2)
I_K	density of K current (μA/cm^2)
I_L	density of leakage current (μA/cm^2)
I_{Na}	density of Na current (μA/cm^2)
I_m	density of membrane current (μA/cm^2)
i_i	total ionic current (μA)
i_{mj}	membrane current at segment j (μA)
i_{ej}	injected current at segment j (μA)
j	number of segment $j = 0, \ldots, J+1$
k	number of time steps (Δt) beginning at time of current injection
$[K]_0$	outside K concentration at rest (3·1 mM)
$[K]_{oj}^k$	outside K concentration at segment j at time interval k
m	Hodgkin & Huxley variable describing Na activation
n	Hodgkin & Huxley variable describing K activation
R	axoplasmic specific resistance (90 Ω cm)
r_j	axoplasmic resistance per cm length of segment ($r_j = R/\pi a_j^2$)
t	time (msec)
V_K	K equilibrium potential (-12 mV)
V_L	leakage equilibrium potential (10·598 mV)
V_m	membrane potential (mV) ($V_m = 0$ at rest)
V_{Na}	Na equilibrium potential (115 mV)
$\dot{V}$	dV/dt
x	distance from point of current injection
λ	axon space constant (cm)
θ	thickness of the periaxonal space (cm)
τ_K	time constant of recovery process reducing extracellular K concentration to the resting level (msec)
Δt	time integration step (msec)
Δx_j	length of segment j (cm)

Equations

Khodorov, Timin, Vilenkin & Gul'ko (1969) and Khodorov, Timin, Pozim & Shemelev (1971), using the method of Cooley & Dodge (1966), describe a mathematical model for the propagation of a single action potential and trains of impulses at high frequencies through a step increase in axonal diameter. Parnas *et al.* (1976) expanded the model to include gradual changes in axon diameter and changes in extracellular concentration of K. The same approach is used in this paper; therefore, the mathematical description, already published in detail (Cooley & Dodge, 1966; Khodorov *et al.* 1969; Parnas *et al.* 1976) has not been repeated. In this section we emphasize only modifications to the previous methods and present the solution for the branch point (see Appendix).

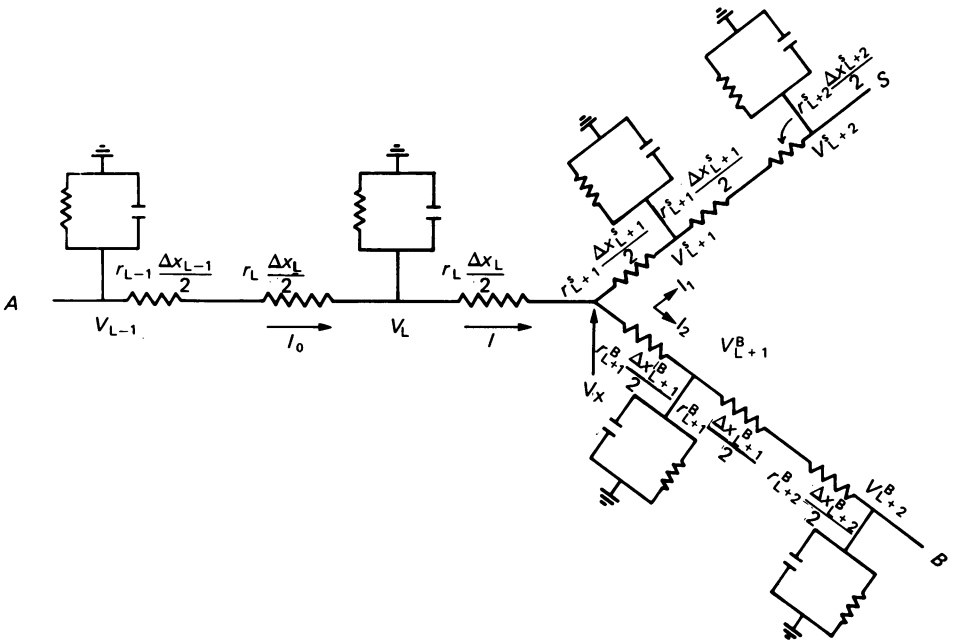

Fig. 1. Equivalent circuit of a bifurcation in axon. The branch point is at segment L and the segment length Δx_j is variable. Branch A represents the parent branch, S and B the daughter branches.

The initiation and propagation of the nerve impulse was described by Hodgkin & Huxley (1952) showing the membrane current to be

$$I_m = \frac{a}{2R}\frac{\partial^2 V}{\partial x^2} = C\frac{\partial V}{\partial t} + \bar{G}_{Na} m^3 h(V - V_{Na}) + \bar{G}_K n^4 (V - V_K) + G_L(V - V_L). \quad (1)$$

This equation was used in all the theoretical works where the axon was considered to be composed of series connected segments (Cooley & Dodge, 1966; Khodorov *et al.* 1969; Dodge & Cooley, 1973). While Parnas *et al.* (1976) treated the theoretical axon as composed of segments with varying radii (a_j) and a constant length (Δx) we introduce here a variable segment length (Δx_j). This was done in order to establish a stable solution which is independent of the diameter of the axon's branches (see Results).

In the case of a bifurcating axon, Fig. 1, the parent branch (A) bifurcates at segment L into two daughter branches: S (small branch), B (large branch). The bifurcation was taken at the point x, where

$$x = \sum_{j=0}^{L} \Delta x_j + \frac{\Delta x_L}{2}.$$

The lumped equivalent circuit corresponding to these conditions is shown in Fig. 1. From the equivalent circuit we can derive an appropriate finite difference approximation to eqn. (1):

From Kirchoff's law the membrane current at the branching segment L (Fig. 1) is

$$i_{mL} = C_L \cdot \dot{V}_L + i_{iL} = \frac{V_{L-1} - V_L}{\frac{1}{2}\Delta x_{L-1} \cdot r_{L-1} + \frac{1}{2}\Delta x_L \cdot r_L} - I, \tag{2}$$

where

$$I = \frac{V_L - V_x}{\frac{1}{2}\Delta x_L \cdot r_L} = \frac{V_x - V^S_{L+1}}{\frac{1}{2}\Delta x^S_{L+1} \cdot r^S_{L+1}} + \frac{V_x - V^B_{L+1}}{\frac{1}{2}\Delta x^B_{L+1} \cdot r^B_{L+1}} \tag{3}$$

and V_x is the potential at the point of branching. Since

$$V_x = V_L - I \cdot \tfrac{1}{2}\Delta x_L \cdot r_L$$

by substituting V_x in eqn. (3), solving for I, we get $\dot{V}_L$ from eqn. (2):

$$\dot{V}^k_L = \frac{1}{C}\left\{\frac{a_L}{R \cdot \Delta x^2_L}\left[D_{L-1} \cdot V^k_{L-1} - (D_{L-1} + Z^S_{L+1} + Z^B_{L+1})\, V^k_L + Z^S_{L+1} \cdot V^{Sk}_{L+1} + Z^B_{L+1} \cdot V^{Bk}_{L+1}\right] + \frac{i^k_{SL}}{2\pi a_L \cdot \Delta x_L} - G^k_L (V^k_L - U^k_L)\right\}, \tag{4}$$

where G^k_L and U^k_L are as defined in Parnas *et al.* (1976) for $j = L$. Z^S_{L+1} and D_{L-1} are given by

$$Z^S_{L+1} = \frac{a^{S^2}_{L+1}}{\Delta x^S_{L+1}} \Big/ \left(\frac{a^2_L}{\Delta x_L} + \frac{a^{S^2}_{L+1}}{\Delta x^S_{L+1}} \frac{a^{B^2}_{L+1}}{\Delta x^B_{L+1}}\right); \quad D_{L-1} = \frac{1}{1 + (\Delta x_{L-1}/\Delta x_L) \cdot (a_L/a_{L-1})^2} \tag{5}$$

and Z^B_{L+1} is obtained by exchanging S and B in eqn. (5). For integration with respect to time, we used the Euler method as the predictor

$$V^{k+1}_j = V^k_j + \Delta t \cdot \dot{V}^k_j \tag{6}$$

and the modified Euler method as the corrector:

$$V^{k+1}_j = V^k_j + \tfrac{1}{2}\Delta t (\dot{V}^k_j + \dot{V}^{k+1}_j) \tag{7}$$

with similar equations for m, h and n (Hodgkin & Huxley, 1952).

The numerical solution for the equation (given in the Appendix) was programmed in FORTRAN and used Gerber scientific model 23 for the graphic output.

RESULTS

(A) *Stability of the numerical solution*

Most of the numerical solutions of Hodgkin & Huxley equations were computed for an axon with a radius equal to that of the squid axon (238 μm) (Khodorov *et al.* 1969). In these cases, a stable numerical solution was obtained by shortening the time and spatial increments (Δt, Δx) (Cooley & Dodge, 1966; Moore & Ramon, 1974; Moore, Ramon & Joyner, 1975). For evaluation of the solution accuracy, comparison between action potential shape, duration and velocity was made with successively smaller Δx, Δt, until the solution became independent of size of the time and space increments (a 'correct' solution). It was found that for the squid axon parameters, the modified Euler method yields a 'correct' solution for constant $\Delta x = 500\,\mu$m and $\Delta t \leqslant 0{\cdot}03$ msec (Moore & Ramon, 1974).

Since we used axons with different branch diameters, it was necessary to find out which Δx_j and Δt values yield a 'correct' solution for the changing diameters a_j values. We found that when Δt was smaller than or equal to 0·03 msec, a stable solution was obtained independent of branch diameter. In Fig. 2 comparison between action

potentials obtained for three segment lengths is shown. Δt was kept constant at 0·03 msec. When $\Delta x = \lambda/2$, the action potential (voltage) seemed normal, although it had a shorter delay and higher amplitude than those obtained with smaller Δx values ($\lambda/4$ and $\lambda/10$). However, the solution for the membrane current (I_m) with $\Delta x = \lambda/2$ had unacceptable oscillations during its negative peak (Fig. 2, bottom traces). Thus it appears that the membrane current is a much more sensitive test for the accuracy of the numerical solution than the membrane potential. It was found that for all axon diameters, the same accuracy was obtained when $\lambda/\Delta x$ equalled 10 or more. Therefore, in all of our computations Δx_j were always taken as $\lambda/10$ according to the diameter of each branch. Δt was always taken as 0·03 msec.

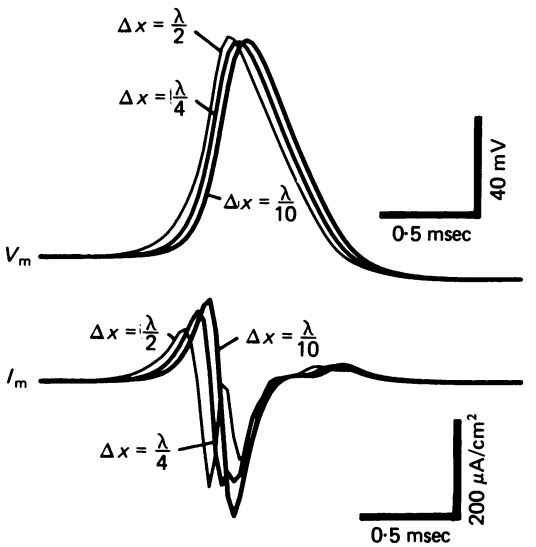

Fig. 2. Comparison of numerical solution of the propagated action potentials (upper trace) and membrane currents (lower trace) for three segment lengths Δx. For $\Delta x \leqslant \lambda/10$ both membrane potential and current are stable. The integration time step is 0·03 msec for all three cases.

(B) *The effects of the geometrical ratio*

The effects of branch diameter upon action potential propagation was computed using the geometrical ratio criterion (GR) developed by Rall (1959, 1962, 1964). The geometrical ratio is defined as

$$GR = \frac{a^{S^{\frac{3}{2}}} + a^{B^{\frac{3}{2}}}}{a^{\frac{3}{2}}},$$

where a is the radius of the parent axon and a^S, a^B that of the daughter branches. If it is assumed that R_m, R and C are uniform for all branches and that each branch is at least several λ in length, a transformation between a branching axon and an axon with a step change in axon diameter (equivalent cylinder) is possible (Goldstein & Rall, 1974).

Fig. 3 shows the effect of different GR values on single action potential and membrane current one segment (0·1 λ) before (left in each column) and after (right in each column) the branch point. We found that the action potentials and currents in both daughter branches S and B are the same and independent of branch diameters (Fig. 3, each right column is composed of superposition of the responses in the two daughter branches).

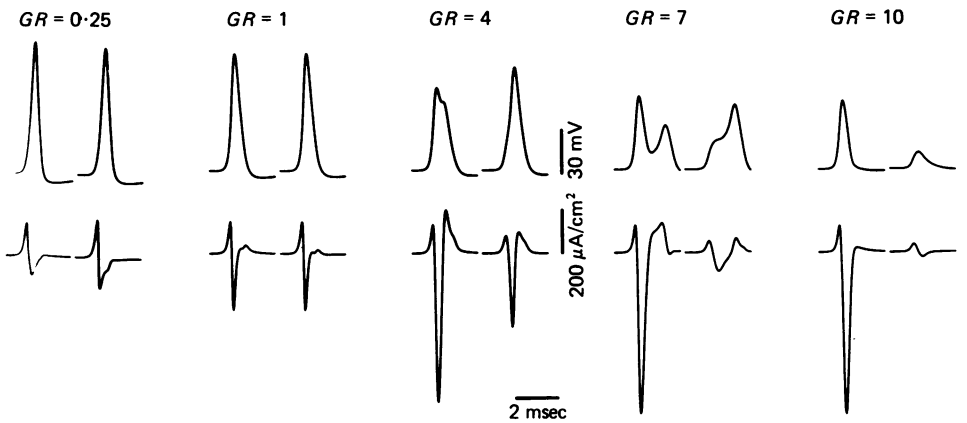

Fig. 3. Behaviour of action potentials (upper trace) and membrane currents (lower trace) near the branch segment at five different GR. At each GR, the left column shows the shape of the action potential and its membrane current, 0·1λ before the branching point and the right column is a superposition of the 'records' obtained 0·1λ after the branch point at *both* daughter branches S and B. At $GR = 10$, the action potential fails to propagate at the segment of branching.

When $GR = 1$, the response before and after the bifurcation is the same as for an homogeneous axon ($V_m = 86\,\text{mV}$, $I_m = 260\,\mu\text{A/cm}^2$). For the case of $GR = 0{\cdot}25$ (narrowing), the amplitude of the action potential is increased both before and after the bifurcation. There are also differences in the currents before and after the bifurcation, the negative phase being smaller in comparison to the case where $GR = 1$.

When $1 < GR < 10$ (widening up to 4·6 times), the action potential before the branch point is smaller and has an additional peak on its falling phase, due to a 'reflexion' from the post-bifurcation region (see Khodorov *et al.* 1969; Parnas *et al.* 1976). In these cases, a large negative and second positive phase in the membrane currents were observed and propagation through the branch point is delayed. As GR increases, the 'reflexion potential' grows and is accompanied by large positive membrane current.

In the case of $GR = 10$ (widening $\simeq$ 4·6 times), propagation into *both* branches failed at the same time and the reflexion potential and the second positive phase of the membrane current disappeared (note that the current beyond the branch point is biphasic, Noble, 1966).

We would like to emphasize again that for each constant geometric ratio, changes in the diameter ratio of the daughter branches never yield differential conduction into the two daughter branches. Either both branches showed propagating action potentials or conduction failed in both. These theoretical computations are therefore not in accord with the experimental findings (Grossman *et al.* 1979*a*).

(C) *Effects of periaxonal K concentration*

During repetitive activity of an axon the extracellular K concentration in the periaxonal space is increased (Frankenhaeuser & Hodgkin, 1956; Baylor & Nicholls, 1969). In this section, we incorporate changes in $[K]_o^k$ according to the following equation (Parnas *et al.* 1976):

$$[K]_{oj}^k = [K]_o + ([K]_{oj}^{k-1} - [K]_o) . e^{-t/\tau} \tau_K + I_{Kj}^{k-1} . \Delta t / F\left(\theta + \frac{\theta^2}{2a}\right), \quad (8)$$

where

$$I_{Kj}^k = G_{Kj}^k (V_j^k - V_{Kj}^k).$$

From this we calculate V_{Kj}^k, the changing K battery:

$$V_{Kj}^k = \frac{RT}{F} \ln \frac{[K]_{oj}^k}{[K]_i},$$

where the internal K concentration $[K]_i$ was taken as a constant. (Since $\theta \gg \theta^2/2a$ Parnas *et al.* (1976) omitted in their equation the term $\theta^2/2a$.)

The accumulation of K outside an axon will depend on the thickness of the periaxonal space (θ) and the rate at which accumulated K is removed (τ_K). There can be considerable variability in the spacing of the glial layers surrounding the axon membrane; in some axons glial cells were missing altogether around some of their branches (Castel, Spira, Parnas & Yarom, 1976). There also can be differences in the efficiency of the recovery processes. For example, in the leech the activity of one important mechanism for K removal, the electrogenic Na pump, varies among different cells and even between branches of a single cell (Van Essen, 1973; Jansen & Nicholls, 1973). Therefore, we let θ (θ^S, θ^B), the thickness of the periaxonal space, vary from 150 to 600 Å and τ_K (τ_K^S, τ_K^B), the time constant of recovery vary from 10 to 50 msec and then studied the effects on potassium accumulation and propagation through a bifurcation. In these computations we also used the α_h and β_h of Hodgkin & Huxley, as modified by Adelman & Palti (1969), to account for additional effects of K on sodium inactivation. In order to economize in computer time, we used stimulation frequencies of 300 Hz as did Parnas *et al.* (1976) and which are higher than those used in the actual experiments (Grossman *et al.* 1979*a*).

(*a*) *Case of identical periaxonal space and identical rate of K removal for both the daughter branches*

Again, the main finding is that when $\tau_K^S = \tau_K^B$ and $\theta^S = \theta^B$, no differences in the behaviour of S and B branches were seen, no matter what the ratio a^B: a^S was (Fig. 4*A*). (Since in eqn. (8) $\theta^2/2a \ll \theta$, the extracellular concentration is almost independent of the axon diameter. With $\theta = 300$ Å, after 10 impulses at 300 Hz, a difference of only 0·1 mM in the extracellular K concentration was found between two axons with diameter ratio of 1 : 10. These differences caused the tenth spike to be 0·1 mV *smaller* in the *thick* axon than in the thinner one.)

We found that the accumulation of K in the periaxonal space greatly affected the behaviour of action potentials at the branch point. In some cases extracellular K accumulation at such a region could block the propagation that otherwise could pass through the bifurcation (see also Parnas *et al.* 1976). In Fig. 4*B* an example of the

combined effect of $GR > 1$ and K accumulation is shown. While in the case of $GR = 5$, when K accumulation was not permitted, only the fourth action potential failed at the branch point (not shown), when K accumulation is allowed, the second action potential also failed to propagate beyond the branch point. The absence of the second peak on the falling phase of the second and the fourth action potentials one segment before the branch point (Fig. 4*B*, segment 30*A*) is also an indication of this failure.

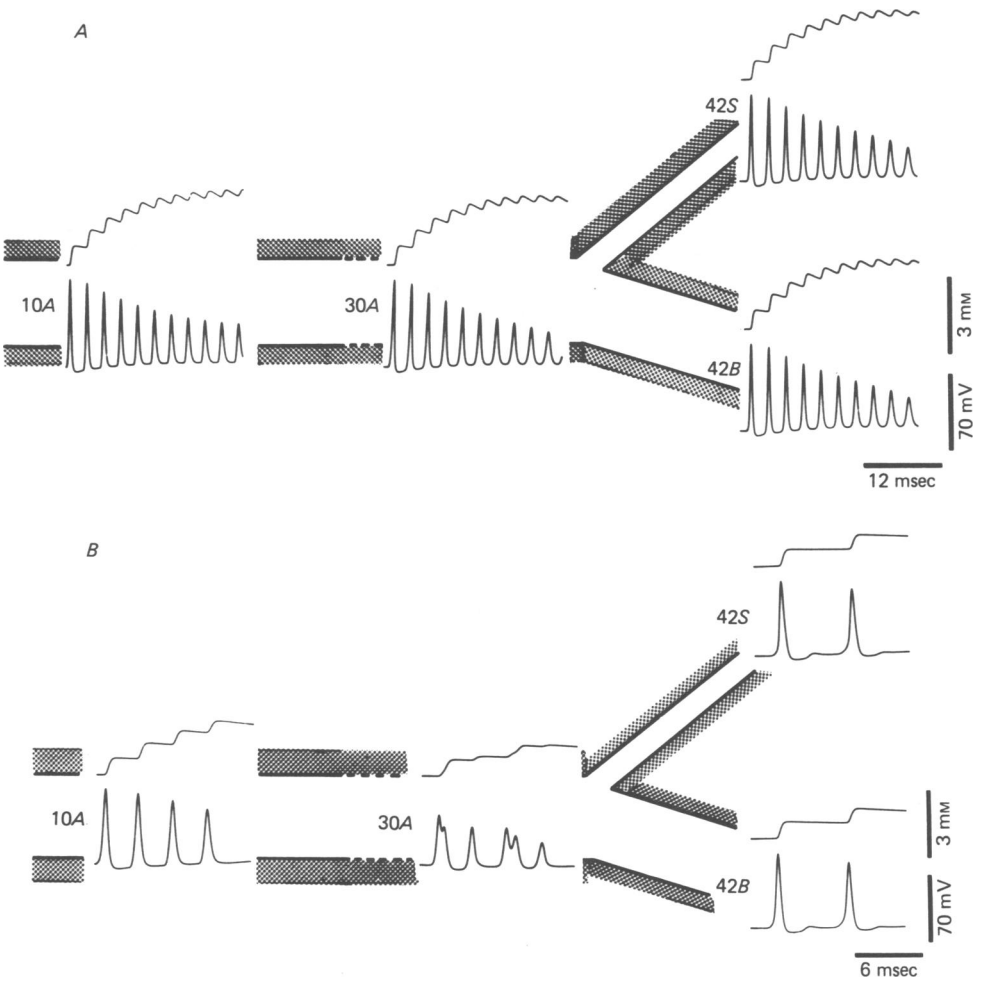

Fig. 4. Effects of K accumulation in the periaxonal space on train of action potentials propagating along a bifurcating axon at a frequency of 300 Hz. At each segment, upper trace shows the periaxonal K concentration beginning from 3·1 mM at rest. Lower traces show membrane potential. Dotted area marks the periaxonal space. 'Recording' segments are given near traces. *A*, constants used: $GR = 1$, $\tau_K = \tau_K^S = \tau_K^B = 20$ msec.

$$\theta = \theta^S = \theta^B = 400\,\text{Å}.$$

No differential behaviour between the daughter branches can be seen. *B*, constants used: $GR = 5$, $\theta = 600$ Å, $\theta^S = \theta^B = 300$ Å, $\tau_K = \tau_K^S = \tau_K^B = 20$ msec. Notice that due to the increase in GR and the periaxonal K accumulation, the second and fourth spikes fail to propagate beyond the point of branching, but no differential behaviour between the daughter branches is seen.

(*b*) *Case of different radial thickness of the periaxonal space*

In Fig. 5*A*, a typical example is shown of a train of four impulses in a bifurcating axon ($GR = 1$) with different peribranch space ($\theta^S = 600$ Å and $\theta^B = 150$ Å). Such a difference in θ produced 2·6 mM more extracellular K concentration after the fourth action potential in the branch *B*. The result of such concentration differences can be seen by comparing the responses in segment 52*S* and segment 52*B*. In segment 52*S*,

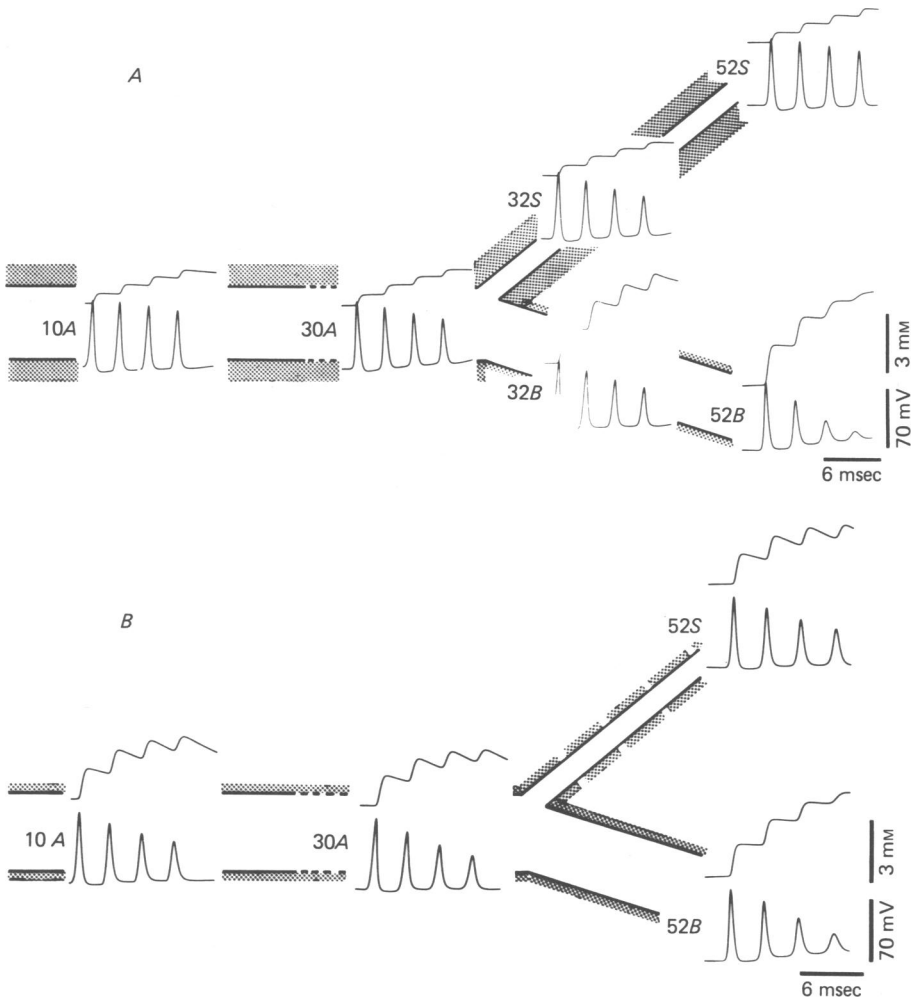

Fig. 5. Effects of K accumulation in the periaxonal space on the behaviour of four action potentials propagating along bifurcating axon where the daughter branches have different periaxonal spaces (*A*) or different rates of recovery (*B*). In *A*, $GR = 1$,

$$\tau_K^S = \tau_K^B = 20 \text{ msec}, \quad \theta^B = 150 \text{ Å}, \quad \theta^S = 600 \text{ Å}.$$

Notice that the third and the fourth spike fail to propagate to the *B* branch (small periaxonal space), while all four propagate in the *S* branch (see text). In *B*, $GR = 1$, $\theta = \theta^S = \theta^B = 200$ Å, $\tau_K = \tau_K^S = 10$ msec and $\tau_K^B = 50$ msec. Notice that the fourth action potential is smaller in the *B* branch due to the slower recovery process at this branch. In branch *S* openings in the periaxonal space indicate faster recovery processes.

four propagating action potentials can be seen while in 52*B* only the first two action potentials propagated. The third and fourth responses declined with distance. Thus, several space constants away from the branch point, four action potentials appear at branch *S* and only two at branch *B* (not shown).

(c) *Case of different rate of K removal between the daughter branches*

The rate of K removal from the periaxonal space may be controlled by several mechanisms such as the activity of the Na–K electrogenic pump (Jansen & Nicholls, 1973), the permeability of the glial envelope and the rate of K uptake by these cells. We expressed all these and other possible mechanisms which might be different for the two branches under the parameter τ_K.

Fig. 5*B* shows that a branch with a shorter τ_K (τ_K is 10 msec for branch *S* and 50 msec for branch *B*) will respond better than the second branch already after the fourth impulse in a train. Comparison between the fourth action potential in segment 52*B* and that in segment 52*S* shows that it is smaller in the branch with the slower τ_K. The differences in recovery time affect propagation less than the differences in periaxonal space. It can be seen that even when the recovery ratio was 5 : 1 (50 and

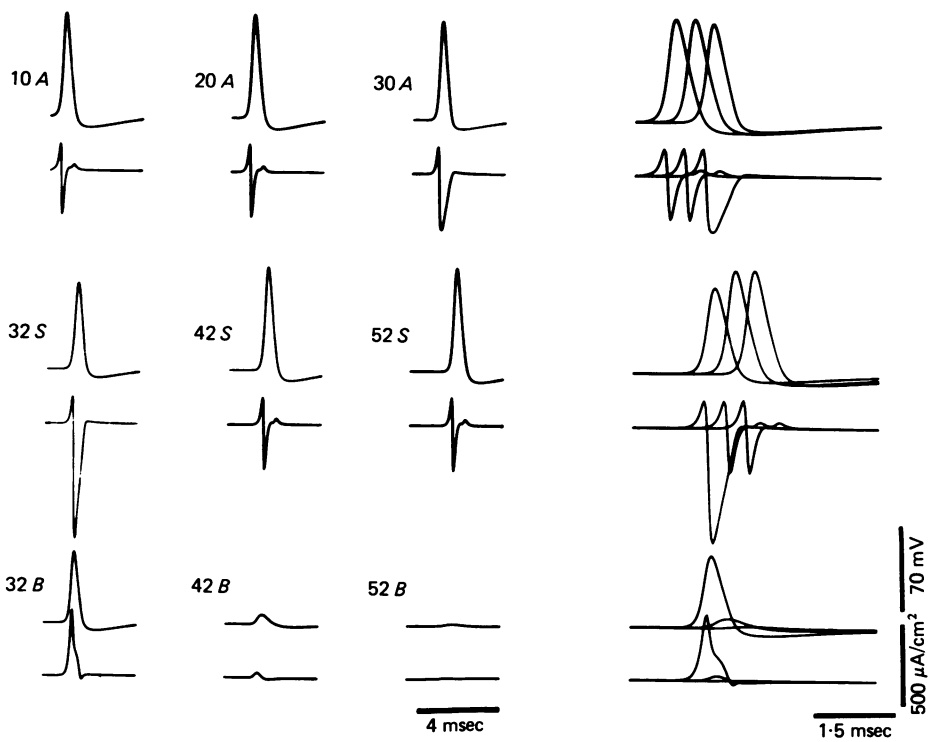

Fig. 6. Effects of an inexcitable daughter branch (*B*) on the propagation of a single action potential along a bifurcating axon. $GR = 1$ and $a^B : a^S = 10 : 1$. Action potential amplitude in 30*A* is 82 mV and in 32*S*, 72 mV. However, in segment 52*S* the action potential appears at its normal height. The plots of each row were superimposed and are given on a faster scale on the right.

10 msec), the differences between the action potentials in the two branches were much smaller than those obtained for the ratio of 4 : 1 (600 and 150 Å) in the radial thickness of the periaxonal space (compare Fig. 5*A* with *B*).

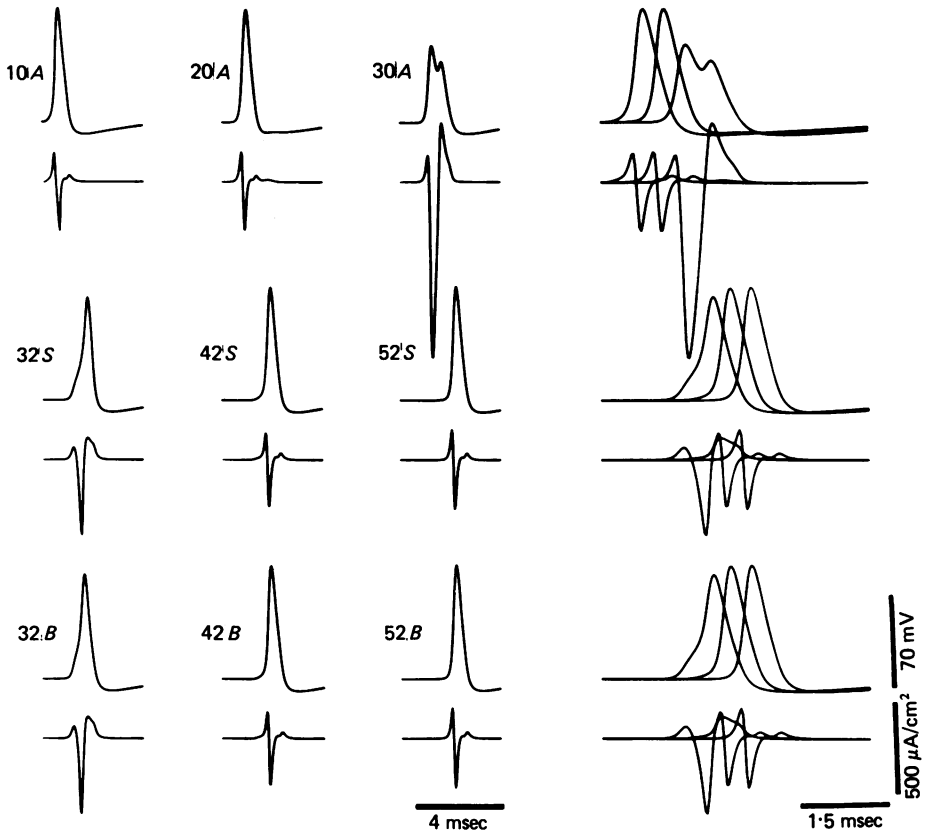

Fig. 7. The behaviour of a single action potential propagating along a bifurcating axon where $GR = 6$ and all branches are excitable. The membrane current at the point near the branch 30*A*, 32*S*, 32*B* is much bigger and longer than at points far from the branch segment.

(d) Effects of inexcitable daughter branch

In a previous article (Grossman *et al.* 1979*a*) it was shown that after high frequency stimulation, conduction of action potentials failed into the thick branch while it continued in the thinner branch. At the stage of the differential conduction, the thicker branch essentially became an inexcitable load for action potentials approaching from the parent branch; thus, the possibility arose that it reduces the safety factor for propagation of action potentials into the thin branch.

An inexcitable daughter branch was simulated by introducing $G^{B^0}_{Na_j} = G^{B^k}_{Na_j}$ (i.e. the Na conductance in the branch *B* remained at its resting value). The dependence of G_K on membrane potential was not changed. In this way, we examined an extreme case where the branch is inexcitable and the increase in G_K due to depolarization

contributes even more to shunting effects. At each GR, we compared the results obtained when the two branches were excitable with those where only one branch was excitable.

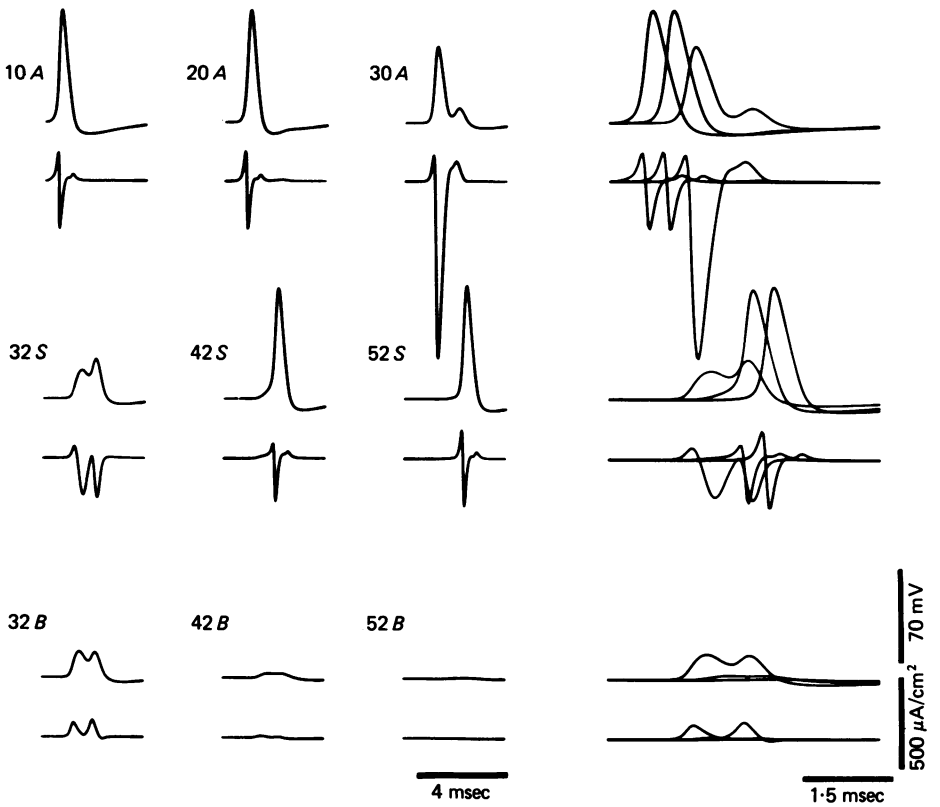

Fig. 8. Same as Fig. 7 but branch B being inexcitable. $a^B:a^S = 2:1$. Comparing with Fig. 7, notice the decrease and the growing delay of the second peak before the bifurcation ($30A$) and the decrease in the outward membrane current at this segment, since now, only the current from the small excitable daughter branch is reflected back to this segment.

Table 1 and Figs. 6–9 summarize the results obtained for cases of $GR = 0{\cdot}25$, 1, 4 and 6. It is clear that although the inexcitable branch affects the amplitude of the action potential before and after the branch point, only in the extreme case where $GR = 6$ and $a^B : a^S = 4 : 1$ does the action potential fail to propagate into the normally excitable branch (Fig. 9). In all other cases, the depolarization produced in segment 32 of the excitable branch was sufficient to evoke a full propagated action potential in the more distant segments (Fig. 8, $52S$).

Unlike the case where both branches are excitable, when one branch is inexcitable, the ratio of the diameters of the two daughter branches affects the behaviour of the action potential at the branch region. In general, the effect of the inexcitable branch increases as its diameter increases. For $6 \leqslant GR < 10$ an increase beyond a certain

diameter ratio causes conduction failure at the branch point (4 : 1 in case of $GR = 6$). For $GR = 10$, the conduction failure occurs even when both the daughter branches are excitable (see section B).

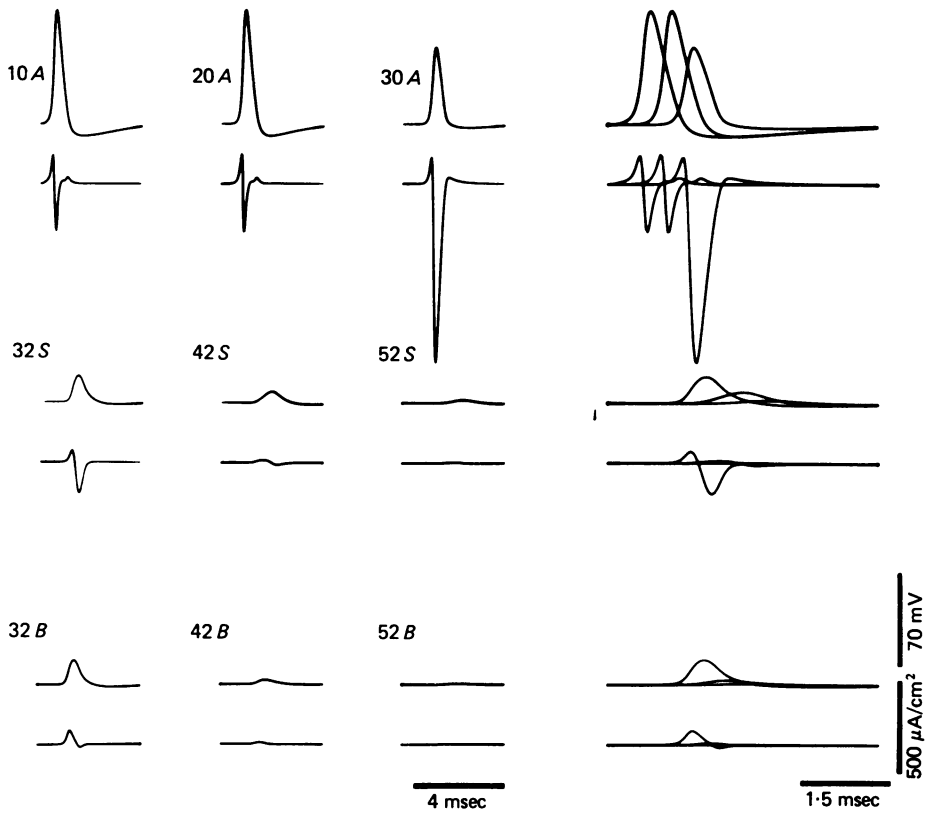

Fig. 9. Same as Fig. 8 but $a^B : a^S = 4 : 1$. In this case the action potential fails to propagate to the excitable daughter branch S. The second peak before the branch disappears and only small inward current can be seen at $32S$ which decays electrotonically along this branch. Compare currents in $32S$ (excitable) and $32B$ (inexcitable).

Examining the case of $GR = 1$ in more detail (Fig. 6 and Table 1), we again found that the current is a more sensitive criterion for detecting a lack of homogeneity at the branch point. The maximal effect at $GR = 1$ occurs when the ratio $a^B : a^S$ is 10 : 1. In this case, the action potential, one segment before the branch, falls to 82 mV (from 86 mV) in the excitable S branch. However, the negative peak of the membrane current at these segments dramatically increased (from 260 to 334 μA/cm^2 before the branch point, and to 680 μA/cm^2 after the branch). At the same time, the current seen in the inexcitable branch was mainly outward and biphasic, as seen in the experimental results (Grossman *et al.* 1979*a*).

An interesting finding was noted when we compared Figs. 7–9. All Figures describe a case of $GR = 6$. In one case both daughter branches were excitable (Fig. 7). In the others, B branch was inexcitable and the ratio of $a^B : a^S$ was 2 : 1 (Fig. 8) and 4 : 1

(Fig. 9). In Figs. 7 and 8, where the action potential propagated beyond the branch point, the action potential one segment before the branch is composed of two peaks (Figs. 7, 8, at 30 A). In the case (Fig. 9) where the action potential did not propagate across the branch, the second peak is missing (Fig. 9, top 30 A). Nevertheless, the first peak of the action potential in all three cases is the same (58 mV, Table 1), showing that this response is not affected by the nature of the post-branch response or diameter ratios at that *GR*. The second peak decreased and appeared after a longer delay as the diameter of the inexcitable branch increased (see Discussion).

TABLE 1. The effect of an inexcitable daughter branch (*B*) on the height of a propagating action potential 0·1λ before the branching point (30*A*) and 0·1λ after the branching point in the excitable branch (32*S*). Results for the case where all branches are excitable are given in top row. Bold number (lower right corner) indicates block of conduction in branch *S*

	GR = 0·25		*GR* = 1		*GR* = 4		*GR* = 6		
	Spike height (mV)		Spike height (mV)		Spike height (mV)			Spike height (mV)	
$a^B : a^S$	30*A*	32*S*	30*A*	32*S*	30*A*	32*S*	$a^B : a^S$	30*A*	32*S*
All branches excitable	95	91	86	86	65	81		58	78
10 : 1	93	87	82	72	64	37	1 : 1	58	55
100 : 1	93	87	82	72	64	35	2 : 1	58	29
1000 : 1	93	87	82	72	64	35	3 : 1	58	20
							4 : 1	58	**19**

Another interesting finding can be seen in Fig. 8 at segment 32*S* where the membrane current shows *two* negative phases. The delay between these two negative peaks, which indicate Na inward current, is short and seems to be in the absolute refractory period of the axon (see Discussion).

In general, it seems that an inexcitable branch has little effect on the safety factor for propagation of action potentials across the bifurcation. Only in extreme cases can its presence cause a complete block of propagation at this region.

DISCUSSION

The present computations were not aimed at obtaining an accurate simulation of the experimental results given in the preceding articles (Grossman *et al.* 1979*a*, *b*). Rather, they give a quantitative description of the conduction of action potentials at high frequency under a given arbitrary set of conditions. Many of the parameters required for accurate simulation are not known for the axons of *Panulirus*. We therefore used parameters which are known for the squid axon (Hodgkin & Huxley, 1952; Adelman & Palti, 1969) or the cockroach axon (Parnas *et al.* 1976). In some computations, which are not shown in the present article, we varied some of the parameters such as $[K]_o$, $\bar{G}_{Na}$ or *R* and found that the differences obtained were not significant and were expressed in the rate at which the block of conduction was obtained. In the case where we took $[K]_o$ as 12 mM, as given in the experiments (Grossman *et al.*

1979*b*), and using the Adelman & Palti (1969) expression, even conduction of single action potentials was suppressed (probably because of incompatibility of other parameters). We therefore used the value of $[K]_0 = 3{\cdot}1$ mM as in the previous computations (Parnas *et al.* 1976).

While searching for Δx and Δt values that give a stable solution for the propagating Hodgkin & Huxley action potential, using the modified Euler numerical method, we found that the spatial integration step must be smaller than $\lambda/10$ of the axon. This result is important for investigators modelling action potentials propagating along inhomogeneous axons. It is necessary to choose $\Delta x < \lambda/10$ for each homogeneous part of the axon (or to take the smallest Δx for the whole axon). We also found that the membrane current, due to its fast transients, provides a very sensitive test for the accuracy of the numerical solution. The action potential shape and amplitude, on the other hand, are much less affected by the integration step size (Moore, Ulbricht & Takata, 1964; Khodorov, Timin, Vilenkin & Gul'ko, 1970).

The membrane current also provides a sensitive indicator for regions of axonal inhomogeneity. At regions of low safety factor for spike propagation (such as abrupt widening, branching with $GR > 1$, or a bifurcation with an inexcitable branch), the action potential shows relatively small changes while the changes in membrane current before and after such regions are much more noticeable (Fig. 3 and Figs. 6–8). Furthermore, the potential can be very similar in branches with different excitabilities while their currents greatly differ (compare segments $32S$ with $32B$ in Fig. 6 and in Fig. 9). This phenomenon can also be seen in the experimental findings of Grossman *et al.* (1979*a*). Comparison between the action potential in the parent axon before and after block of conduction into the thick branch shows only small differences in shape; on the other hand, there was a marked reduction in the size of the membrane current.

One of the interesting results obtained in the present computations is the change in the shape and amplitude of the membrane current in the segment just before a branch ($GR > 1$) or a region of inhomogeneity. Specifically we would like to emphasize the increase in the *inward* membrane current phase seen near the branch point (Fig. 6, $32S$; Fig. 7, 30 A) or in general near a region of a low safety factor. The relation between the amplitude of an action potential and membrane current at region of low safety factor has been discussed in detail by Khodorov & Timin (1975). Thus, it is possible to obtain different membrane currents at different regions of an axon even though the maximal sodium conductance ($\bar{G}_{Na}$) per cm^2 and all other Hodgkin & Huxley parameters are the same. A corollary of these computations is that the amplitude or rise time of the action potential does not always reflect that of the membrane current.

The main purpose of our computation was to find out the minimal necessary assumptions for which differential flow of impulses into the daughter branches occurs. We found that axon geometry (i.e. branch diameter) alone *could not* account for such a 'filtering' (Fig. 4).

A geometrical difference that can result in differential conduction into the two branches is the thickness of the periaxonal space which will influence the K concentration around the axon. However, difference between peribranch spaces was not found experimentally in the lobster (Grossman *et al.* 1979*b*) although it was found in the cockroach (Castel *et al.* 1976). Another difference may be in the rate at which the accumulated K is removed. Such differences may be due to variations in the density

of the glial envelope or in preferential activation of an electrogenic pump. This may be caused by differences in the internal ionic concentration between the small and large daughter branches after high frequency stimulation (Paintal, 1965). It is concluded that any mechanism which will introduce differences in the K concentration around the daughter branches provides a possible explanation for preferential conduction into one branch, especially if direct effects of K on excitability take place.

When conduction into one branch was blocked, that branch in effect became an inexcitable load for the approaching action potential. It was surprising how little such an inexcitable branch affected the propagation near the branch point.

In cases where $GR < 6$, increasing the ratio between the radii of the inexcitable branch (a^B) and the excitable one (a^S) beyond a certain value did not decrease the safety factor at the bifurcation (Table 1). In case of $GR = 1$, for example, there were no further changes in action potential, shape and velocity at this region when $a^B : a^S$ was increased beyond 10 : 1.

In the case of $GR = 1$, when $a^B : a^S = 10 : 1$, the radius of the parent branch is only 3 % bigger than that of the inexcitable one. Since the radius of the daughter branch cannot exceed that of the parent branch for $GR = 1$, further increase in $a^B : a^S$ can have little effect on the diameter of the inexcitable daughter branch. At the same time, the diameter of the excitable daughter branch decreases and thus less current is needed to initiate action potential at this branch. The shunting effect of an inexcitable branch, for $GR < 6$, is sufficiently small that enough current spreads from the parent branch to the excitable daughter branch and propagation to this branch continues.

Only for $6 \leqslant GR < 10$ are there ratios between the radii of the daughter branches such that the fall in the safety factor caused by both the widening ($GR > 1$) and the presence of an inexcitable branch is enough to block the conduction at the branch point. As was mentioned before, for $GR \geqslant 10$, conduction failure is seen even for the case where both branches are excitable (Fig. 3). At any case, an inexcitable branch is a *small* shunt and causes conduction failure in the branch segment only in extreme cases (Fig. 9). Therefore inexcitability of dendrites cannot be an immediate explanation for conduction failure at least in the cockroach (Yarom, 1978).

It is interesting to note that one of the daughter branches may act as a large shunt and will significantly reduce the safety factor at the branch segment, if a synapse is localized at this branch near the bifurcation. Since the membrane resistance is much greater than the axoplasmic one, a synapse which will reduce the membrane resistance without reaching the threshold might have a dramatic effect on the conduction near the branch (Spira *et al.* 1976; Castel *et al.* 1976).

Another interesting result was obtained in the computations for a bifurcating axon with $GR = 6$ and one inexcitable branch. The membrane current appears with two negative phases just past the branch point (Fig. 8, $32S$). This is surprising because the interval (0·66 msec) between these negative peaks which represent Na inward current is small compared with the absolute refractory period (2 msec). Examining Hodgkin & Huxley (1952) variables from the computer output for this segment (not shown), we found that since the action potential before the branch point is small, the inactivation factor, h, decreased only to 0·4 during the first peak of the action potential (and not to nearly zero as in the normal case). Under these conditions the depolarization produced by the potential reflected from segment $42S$ is sufficient to trigger a second peak of inward sodium current in segment $32S$ (Segev, 1976). This might be

a mechanism for 'back firing' in region of axonal inhomogeneity (Howe, Calvin & Loeser, 1976; Calvin & Hartline, 1977). Re-excitation of the normal trigger zone of the axon initial segment by the retrogradely invading action potential of the soma-dendritic region is suggested to be the mechanism of the double action potentials observed in many types of neurones (Calvin, 1978).

Two main phenomena were observed experimentally at the bifurcating axons: (*a*) the differential channelling of action potentials into the daughter branches of a single axon (Grossman, Spira & Parnas, 1973; Grossman *et al.* 1979*a*, *b*); and (*b*) the total conduction block of action potentials at the branch segment (Parnas,1972; Grossman *et al.* 1973; Yau, 1976). The preferential effect could not be explained simply on the basis of diameter differences between the daughter branches unless we assume that because of diameter differences the intracellular ionic concentration in the two branches varies after high frequency stimulation. Such differences could preferentially activate electrogenic pumps in these branches (review by Parnas, 1979; Grossman *et al.* 1979*b*). Otherwise one must assume additional factors in order to explain the differential channelling into the daughter branches (Goldstein & Rall, 1974). Such mechanisms may be geometrical differences in the peribranch spaces or in the excitability of the daughter branches (Zeevi, 1972).

The conduction block at the bifurcation may be explained on a geometrical basis in cases where $GR > 10$ (Fig. 3). For cases where $6 \leqslant GR < 10$, a presence of an inexcitable daughter branch may provide an explanation for the blocking effect of the branch region. However, for cases where $GR < 6$, additional factors are needed to explain the conduction failure at the branch point. Grossman *et al.* (1973, 1979*a*) observed such a failure at the lobster giant axon where $GR = 1$, and branches being excitable. They also showed that the block occurred at the branch point *per se* and not along the branches. Our computation shows that for the case of $GR = 1$, a block will occur along the whole axon, and not only at the branch point (Fig. 4). Thus we assume that some factors exist which affect only the branch region and not regions away from it. For example, one may assume that the branching region is composed of a membrane which is excitable to a lesser degree than the membrane at the other regions of the axon. Further experimental data are needed in order to tackle the problem of the blocking effect at the branch point where GR is close to 1.

We are grateful to Dr B. Wallace and Dr W. Calvin for reading the manuscript. Supported by grant no. 741 from the United States-Israel Binational Fund.

APPENDIX

For reducing the partial equations of Hodgkin & Huxley into a linear system of equations which describes the propagation of action potentials along a bifurcating axon we used the following procedure: substituting $\dot{V}_L^{k+1}$ from eqn. (4) in eqn. (7) we get

$$A_L^{k+1} \cdot V_L^{k+1} = D_{L-1} \cdot V_{L-1}^{k+1} - Z_{L+1}^S \cdot V_{L+1}^{S\,k+1} - Z_{L+1}^B \cdot V_{L+1}^{B\,k+1} = B_L^{k+1}, \tag{9}$$

where

$$A_L^{k+1} = \frac{R \cdot \Delta x_L^2}{a_L}\left(\frac{2C}{\Delta t} + G_L^{k+1}\right) + D_{L-1} + Z_{L+1}^S + Z_{L+1}^B \tag{10}$$

and B_L^{k+1} as in Parnas *et al.* (1976) for $j = L$.

For the segments $L+1$ we use the same procedure as for segment L: For the branch S we use V_x and Kirchoff's law at the branch point to find I_1, from the expression to $i^S_{m_{L+1}}$ we find $V^{S^k}_{L+1}$ and using it in eqn. (7) we obtain

$$A^{S^{k+1}}_{L+1} \cdot V^{S^{k+1}}_{L+1} - W^S_{L+1} \cdot V^{k+1}_L - W^{SB}_{L+1} \cdot V^{B^{k+1}}_{L+1} - D^S_{L+2} \cdot V^{S^{k+1}}_{L+2} = B^{S^{k+1}}_{L+1}, \tag{11}$$

where

$$W^S_{L+1} = \left(\frac{a_L}{a^S_{L+1}}\right)^2 \cdot \frac{\Delta x^S_{L+1}}{\Delta x_L} \Big/ \left\{1 + \left(\frac{a_L}{a^S_{L+1}}\right)^2 \cdot \frac{\Delta x^S_{L+1}}{\Delta x_L} + \left(\frac{a^B_{L+1}}{a^S_{L+1}}\right)^2 \cdot \frac{\Delta x^S_{L+1}}{\Delta x^B_{L+1}}\right\},$$

$$W^{SB}_{L+1} = \left(\frac{a^B_{L+1}}{a^S_{L+1}}\right)^2 \cdot \frac{\Delta x^S_{L+1}}{\Delta x^B_{L+1}} \Big/ \left\{1 + \left(\frac{a_L}{a^S_{L+1}}\right)^2 \cdot \frac{\Delta x^S_{L+1}}{\Delta x_L} + \left(\frac{a^B_{L+1}}{a^S_{L+1}}\right)^2 \cdot \frac{\Delta x^S_{L+1}}{\Delta x^B_{L+1}}\right\}, \tag{12}$$

$$A^{S^{k+1}}_{L+1} = \frac{R \cdot \Delta x^{S^2}_{L+1}}{a^S_{L+1}} \left(\frac{2C}{\Delta t} + G^{S^{k+1}}_{L+1}\right) + W^S_{L+1} + W^{SB}_{L+1} + D^S_{L+2},$$

where D^S_{L+2} as defined in eqn. (5) for $j = L+1$ and S in the appropriate places, and $B^{S^{k+1}}_{L+1}$ as in Parnas *et al.* (1976) for $j = L+1$ and S as a superscript. Symmetrically for the branch B we get similar equations as (11) and (12) by exchanging B for S.

For the segments $j = 0, \ldots, L-1$ and for $j = L+2, \ldots, J$ the numerical procedures are essentially the same as those of Parnas *et al.* (1976), hence the set of partial equations of Hodgkin & Huxley (1952) is reduced to a linear system of equations

$$A^{k+1}_0 \cdot V^{k+1}_0 - 2D_1 \cdot V^{k+1}_1 = B^{k+1}_0 \quad (j = 0),$$

$$A^{k+1}_j \cdot V^{k+1}_j - D_{j-1} \cdot V^{k+1}_{j-1} - D_{j+1} \cdot V^{k+1}_{j+1} = B^{k+1}_j \quad (j = 1, \ldots, L-1),$$

$$A^{k+1}_L \cdot V^{k+1}_L - D_{L-1} \cdot V^{k+1}_{L-1} - Z^S_{L+1} \cdot V^{S^{k+1}}_{L+1} - Z^B_{L+1} \cdot V^{B^{k+1}}_{L+1} = B^{k+1}_L \quad (j = L), \tag{13}$$

$$A^{S^{k+1}}_{L+1} \cdot V^{S^{k+1}}_{L+1} - W^S_{L+1} \cdot V^{k+1}_L - W^{SB}_{L+1} \cdot V^{B^{k+1}}_{L+1} - D^S_{L+2} \cdot V^{S^{k+1}}_{L+2} = B^{S^{k+1}}_{L+1};$$

$$A^{B^{k+1}}_{L+1} \cdot V^{B^{k+1}}_{L+1} - W^B_{L+1} \cdot V^{k+1}_L - W^{BS}_{L+1} \cdot V^{S^{k+1}}_{L+1} - D^B_{L+2} \cdot V^{B^{k+1}}_{L+2} = B^{B^{k+1}}_{L+1} \quad (j = L+1),$$

$$A^{S^{k+1}}_j \cdot V^{S^{k+1}}_j - D^S_{j-1} \cdot V^{S^{k+1}}_{j-1} - D^S_{j+1} \cdot V^{S^{k+1}}_{j+1} = B^{S^{k+1}}_j;$$

$$A^{B^{k+1}}_j \cdot V^{B^{k+1}}_j - D^B_{j-1} \cdot V^{B^{k+1}}_{j-1} - D^B_{j+1} \cdot V^{B^{k+1}}_{j+1} = B^{B^{k+1}}_j \quad (j = L+2, \ldots, J-1),$$

$$A^{S^{k+1}}_J \cdot V^{S^{k+1}}_J - D^S_{J-1} \cdot V^{S^{k+1}}_{J-1} = B^{S^{k+1}}_J; \quad A^{B^{k+1}}_J \cdot V^{B^{k+1}}_J - D^B_{J-1} \cdot V^{B^{k+1}}_{J-1} = B^{B^{k+1}}_J \quad (j = J),$$

where the boundary conditions are $V^{k+1}_1 = V^{k+1}_{-1}$ (symmetry around the injected point) $V^{S^{k+1}}_{J+1} = V^{B^{k+1}}_{J+1} = 0$ ('dead end').

From the set of eqn. (13) we get by substituting V^{k+1}_j from the j's row to the $j+1$ row a new set of equations, which is used as an algorithm for solving the system (13). For $j = 0, \ldots, L-1$ we get eqn. (10) of Parnas *et al.* (1976).

For $j = L$ we get (dropping the superscript $k+1$ for convenience):

$$V_L = X_L + \Gamma^S_L V^S_{L+1} + \Gamma^B_L \cdot V^B_{L+1}, \tag{14}$$

where

$$\Gamma^S_L = \frac{Z^S_{L+1}}{A_L - D_{L-1} \cdot \Gamma_{L-1}}; \quad \Gamma^B_L = \frac{Z^B_{L+1}}{A_L - D_{L-1} \cdot \Gamma_{L-1}}; \quad X_L = \frac{B_L + D_{L-1} \cdot X_{L-1}}{A_L + D_{L-1} \cdot \Gamma_{L-1}}. \tag{15}$$

For $j = L+1$ we obtain

$$V^S_{L+1} = X^S_{L+1} + \Gamma^{SB}_{L+1} \cdot V^B_{L+2} + \Gamma^S_{L+1} \cdot V^S_{L+2}, \tag{16}$$

where

$$X^S_{L+1} = \frac{R^S_{L+1} + P^S_{L+1} \cdot R^B_{L+1}}{1 - P^S_{L+1} \cdot P^B_{L+1}}; \quad \Gamma^{SB}_{L+1} = \frac{P^S_{L+1} \cdot Q^B_{L+1}}{1 - P^S_{L+1} \cdot P^B_{L+1}}; \quad \Gamma^S_{L+1} = \frac{Q^S_{L+1}}{1 - P^S_{L+1} \cdot P^B_{L+1}}$$

and

$$R^S_{L+1} = \frac{B^S_{L+1} + W^S_L . X_L}{A^S_{L+1} - W^S_L . \Gamma^S_L}; \quad P^S_{L+1} = \frac{W^{SB}_{L+1} + W^S_L . \Gamma^B_L}{A^S_{L+1} - W^S_L . \Gamma^S_L}; \quad Q^S_{L+1} = \frac{D^S_{L+2}}{A^S_{L+1} - W^S_L . \Gamma^S_L}. \quad (17)$$

From symmetry with respect to S and B we get V^B_{L+1}. For $j = L+2, \ldots, J$ we get

$$V^S_j = X^S_j + \Gamma^{SB}_j . V^B_{j+1} + \Gamma^S_j . V^S_{j+1}, \quad (18)$$

where

$$X^S_j = \frac{R^S_j + P^S_j . R^B_j}{1 - P^S_j . P^B_j}; \quad \Gamma^{SB}_j = \frac{P^S_j . Q^B_j}{1 - P^S_j . P^B_j}; \quad \Gamma^S_j = \frac{Q^S_j}{1 - P^S_j . P^B_j}$$

and

$$R^S_j = \frac{B^S_j + D^S_{j-1} . X^S_{j-1}}{A^S_j - D^S_{j-1} . \Gamma^S_{j-1}}; \quad P^S_j = \frac{D^S_{j-1} . \Gamma^{SB}_{j-1}}{A^S_j - D^S_{j-1} . \Gamma^S_{j-1}}; \quad Q^S_j = \frac{D^S_{j+1}}{A^S_j - D^S_{j-1} . \Gamma^S_{j-1}} \quad (19)$$

Thus the system of equations (13) is solved through eqns. (14)–(19) by the algorithm:

$$\begin{aligned}
V^{k+1}_j &= X^{k+1}_j + \Gamma^{k+1}_j . V^{k+1}_{j+1} \quad (j = 0, \ldots, L-1), \\
V^{k+1}_L &= X^{k+1}_L + \Gamma^{S^{k+1}}_L . V^{S^{k+1}}_{L+1} + \Gamma^{B^{k+1}}_L . V^{B^{k+1}}_{L+1} \quad (j = L), \\
V^{S^{k+1}}_j &= X^{S^{k+1}}_j + \Gamma^{SB^{k+1}}_j . V^{B^{k+1}}_{j+1} + \Gamma^{S^{k+1}}_j . V^{S^{k+1}}_{j+1}; \\
V^{B^{k+1}}_j &= X^{B^{k+1}}_j + \Gamma^{BS^{k+1}}_j . V^{S^{k+1}}_{j+1} + \Gamma^{B^{k+1}}_j . V^{B^{k+1}}_{j+1} \quad (j = L+1, \ldots, J-1), \\
V^{S^{k+1}}_{J_0} &= X^{S^{k+1}}_J; \quad V^{B^{k+1}}_J = X^{B^{k+1}}_J.
\end{aligned} \quad (20)$$

For the representation of the theoretical axon we used $J^S = J^B = 100$ and the bifurcating was at the thirty-first segment.

REFERENCES

ADELMAN, W. J., Jr. & PALTI, Y. (1969). The influence of external potassium on the inactivation of sodium current in the giant axon of the squid. *J. gen. Physiol.* **53**, 685–700.

BAYLOR, D. A. & NICHOLLS, J. G. (1969). Change in the extracellular potassium concentration produced by neuronal activity in the central nervous system of the leech. *J. Physiol.* **203**, 555–569.

CALVIN, W. H. (1978). Re-excitation in normal and abnormal repetitive firing of CNS neurons. In *Abnormal Neuronal Discharges*, ed. CHALAZONITIS, N. & BOISSON, M. New York: Raven Press.

CALVIN, W. H. & HARTLINE, D. K. (1977). Retrograde invasion of lobster stretch receptor somata in control of firing rate and extra spike patterning. *J. Neurophysiol.* **40**, 106–118.

CASTEL, M., SPIRA, M. E., PARNAS, I. & YAROM, Y. (1976). Ultrastructure of region of a low safety factor in inhomogeneous giant axon of the cockroach. *J. Neurophysiol.* **39**, 900–908.

COOLEY, J. W. & DODGE, F. A. (1966). Digital computer solutions for excitation and propagation of the nerve impulse. *Biophys. J.* **6**, 583–599.

DODGE, F. A. & COOLEY, J. W. (1973). Action potential of the motoneuron. *IBM J. Res. Develop.* **17**, 219–229.

FRANKENHAEUSER, B. & HODGKIN, A. L. (1956). The after-effects of impulses in the giant nerve fibre of *Loligo*. *J. Physiol.* **131**, 341–376.

GOLDSTEIN, S. S. & RALL, W. (1974). Changes of action potential shape and velocity for changing core conductor geometry. *Biophys. J.* **14**, 731–757.

GROSSMAN, Y., SPIRA, M. E. & PARNAS, I. (1973). Differential flow of information into branches of a single axon. *Brain Res.* **64**, 327–386.

GROSSMAN, Y., PARNAS, I. & SPIRA, M. E. (1979*a*). Differential conduction block in branches of a bifurcating axon. *J. Physiol.* **295**, 283–305.

GROSSMAN, Y., PARNAS, I. & SPIRA, M. E. (1979*b*). Ionic mechanisms involved in differential conduction of action potentials at high frequency in a branching axon. *J. Physiol.* **295**, 307–322.

HODGKIN, A. L. & HUXLEY, A. F. (1952). A quantitative description of membrane current and its application to conduction and excitation in nerve. *J. Physiol.* **117**, 500–544.

HOWE, A. F., CALVIN, W. H. & LOESER, J. D. (1976). Impulses reflected from dorsal root ganglia and from focal nerve injuries. *Brain Res.* **116**, 139–144.

JANSEN, J. K. S. & NICHOLLS, J. G. (1973). Conductance changes, an electrogenic pump and the hyperpolarization of leech neurones following impulses. *J. Physiol.* **229**, 635–655.

KHODOROV, B. I., TIMIN, YE. N., VILENKIN, S. YA & GUL'KO, F. B. (1969). Theoretical analysis of the mechanisms of conduction of a nerve pulse over an inhomogeneous axon. I. Conduction through a portion with increased diameter. *Biofisika* **14**, 304–315.

KHODOROV, B. I., TIMIN, YE. N., VILENKIN, S. YA. & GUL'KO, F. B. (1970). Theoretical analysis of the mechanisms of conduction of a nerve impulse along an inhomogeneous axon. II. Conduction of a single impulse across a region of the fibre with modified functional properties. *Biofisika* **15**, 140–146.

KHODOROV, B. I., TIMIN, YE. N., POZIM, N. Y. & SHEMELEV, L. A. (1971). Theoretical analysis of the mechanisms of conduction of nerve impulses over an inhomogeneous axon. IV. Conduction of a series of impulses through a portion of the fibre with increased diameter. *Biofisika* **16**, 95–102.

KHODOROV, B. I. & TIMIN, YE. N. (1975). Nerve impulse propagation along non-uniform fibres (investigation using mathematical models). *Prog. Biophys. molec. Biol.* **30**, 145–184.

MOORE, J. W., ULBRICHT, W. & TAKATA, M. (1964). Effect of ethanol on the sodium and potassium conductance in the squid axon membrane. *J. gen. Physiol.* **48**, 279–295.

MOORE, J. W. & RAMON, F. (1974). On numerical integration of the Hodgkin and Huxley equations for a membrane action potential. *J. theor. Biol.* **45**, 249–273.

MOORE, J. W., RAMON, F. & JOYNER, R. W. (1975). Axon voltage-clamp simulation. I. Method and tests. *Biophys. J.* **15**, 11–24.

NOBLE, D. (1966). Application of Hodgkin–Huxley equations to excitable tissues. *Physiol. Rev.* **46**, 1–50.

PAINTAL, A. S. (1965). Block of conduction in mammalian myelinated nerve fibres by low temperatures. *J. Physiol.* **180**, 1–19.

PARNAS, I. (1972). Differential block at high frequency of branches of a single axon innervating two muscles. *J. Neurophysiol.* **35**, 903–914.

PARNAS, I. (1979). Propagation in non uniform neurites: form and function in axons. In *The Neurosciences Fourth Study Program*, ed. SCHMITT, F. O. & WORDEN, F. G. Cambridge, Mass.: MIT Press.

PARNAS, I., HOCHSTEIN, S. & PARNAS, H. (1976). Theoretical analysis of parameters leading to frequency modulation along an inhomogeneous axon. *J. Neurophysiol.* **39**, 909–924.

RALL, W. (1959). Branching dendritic trees and motoneurone membrane resistivity. *Expl Neurol.* **2**, 503–532.

RALL, W. (1962). Theory of physiological properties of dendrites. *Ann. N.Y. Acad. Sci.* **96**, 1071–1092.

RALL, W. (1964). Theoretical significance of dendritic trees for neuronal input–output relations. In *Neuronal Theory and Modeling*, ed. REISS, R. F., pp. 73–97. Palo Alto: Stanford University Press.

SEGEV, I. (1976). A mathematical model for the propagation of action potentials along a bifurcating axon. M.Sc. thesis, the Hebrew University, Jerusalem, Israel.

SEGEV, I. & PARNAS, I. (1977). Computer model analysis of possible mechanisms underlying differential channeling of information at bifurcating axons. *Israel J. med. Sci.* **13**, 1145.

SPIRA, M. E., YAROM, Y. & PARNAS, I. (1976). Modulation of spike frequency by regions of special axonal geometry and by synaptic inputs. *J. Neurophysiol.* **39**, 882–899.

VAN ESSEN, D. C. (1973). The contribution of membrane hyperpolarization to adaptation and conduction block in sensory neurones of the leech. *J. Physiol.* **230**, 509–534.

YAROM, Y. (1978). Physiological and morphological differentiation of giant axons during the development of the cockroach *Periplaneta americana*. Ph.D. thesis, Hebrew University, Jerusalem, Israel.

YAU, KING-WAI (1976). Receptive fields, geometry and conduction block of sensory neurones in the central nervous system of the leech. *J. Physiol.* **263**, 513–558.

ZEEVI, Y. Y. (1972). Structural functional relationship in single neurone: SEM and theoretical studies. Ph.D. thesis, University of California, Berkeley, U.S.A.